**Armando Almendarez Camarillo, Norbert Stribeck**

**University of Hamburg**,
Inst. TMC, Bundesstr. 45,D-20146 Hamburg,
Germany

# SAXS Observations of the Oriented Crystallisation of Polyolefines from the Melt

**Abstract**
*In-situ experiments on nanostructure evolution during the oriented crystallisation of polyolenes (polyethylene (PE), polypropylene (PP)) from a highly oriented melt have been carried out by means of synchrotron radiation and small-angle X-ray scattering (SAXS). The general options of data analysis are demonstrated using good data recorded in a study of PE. Mainly we report on the oriented crystallisation of PP from the melt. We report the conditions under which oriented crystallisation is observed. While in our studies of PE we have generally observed two-point diagrams, we include processing conditions for PP, under which a specific four-point diagram is observed with the first two reflections on the meridian and the last two on the equator.*
*On the other hand, a similarity is observed. Under isothermal crystallisation conditions extended crystalline lamellae are formed only during the first minutes, whereas the crystallites formed later remain small. The orientation memory of PP is found to depend strongly on the melt temperature. Its dependence on melt annealing time is low. Because of instrumental problems at the BW4 beam line, HASYLAB Hamburg, our data are too noisy to be used for a quantitative analysis by application of the multidimensional chord distribution function (CDF) method.*

**Key words:** *polyolefines, polyethylene, polypropylene, crystallisation, nanostructure, synchotron radiation, SAXS.*

## Introduction

Understanding polymer crystallisation is central for the tailoring of material properties, and is once more under scientific discussion [1-7]. Nevertheless, the views concerning the evolution of the corresponding semicrystalline nanostructure are still conflicting, because the experimental data collected so far are as yet incomplete. In an earlier paper of this conference series [8], we have demonstrated the prospects of small-angle X-ray scattering from powerful synchrotron radiation sources, regarding the investigation of nanostructure information. It has been pointed out that the advantage of SAXS investigations is greatest if the polymer materials show a high uniaxial orientation.

It seems very difficult by means of imaging methods such as atomic force microscopy (AFM) or scanning near-field optical microscopy (SNOM) to monitor in-situ any structure transfer process executed under technical conditions with sufficient resolution corresponding to both time and space [9-11]. Utilising X-ray scattering, such experiments are possible, but the recorded data require mathematical evaluation, if the application of simplified notions is to be discounted. In order to apply the desired quantitative analysis, we require SAXS patterns with a typical number of 10,000 counts accumulated at the observed peak maxima. At the European Synchrotron Radiation Facility (ESRF) we have carried out such experiments with a cycle time of only 7 s during the oriented crystallisation of polyethylene. Because of the good data quality, we have been able to fully analyse the data [12, 13] and to gain a novel insight concerning the crystallisation process from an oriented melt.

In the study presented here, we intended to process polypropylene in a similar way, and thus to test whether our concept of oriented crystallisation from the melt can be transferred to a different polymer. Unfortunately, at our local beam line at the Hamburg Synchrotron Laboratory (HASYLAB), we did not find the moderate beam conditions that had earlier allowed us to study oriented polyethylene crystallisation quantitatively with a cycle time of at least two minutes [14-16]. Nevertheless, qualitative studies on polypropylene were still possible, and appear worthy of dissemination.

## Experimental section

### Material and setup

Hard-elastic polypropylene films [17] ('Lot #884, as extruded', Celanese, Summit, New Jersey) of 25 μm thickness were stacked with consideration of their high uniaxial orientation to yield samples of 0.8 mm thickness.

Small-angle X-ray scattering (SAXS) was performed in the synchrotron beam line BW4 at HASYLAB, Hamburg, Germany. The wavelength of the X-ray beam was 0.1381 nm. USAXS images were collected by a two-dimensional position-sensitive Gabriel detector (512×512 pixels of $0.4\times0.4mm^2$) (from the European Molecular Biological Laboratory, EMBL). The sample-to-detector distance was set to 12,340 mm.

The samples were wrapped in a single layer of aluminium foil (20 μm thickness), fixed in a frame and subjected to a temperature program using a furnace equipped with two heating cartridges and air cooling provided at the beam line. The image accumulation period was 117 s. Data storage consumes 3 s.

Data from highly oriented polyethylene samples (Lupolen 6021 D, BASF, thickness: 2 mm) from high-pressure injection moulded (HPIM) [18] rods were presented as a reference. They were molten and crystallised in the synchrotron beam of beam line ID02 at the ESRF in Grenoble. The data are recorded using two 2D detectors. In the critical regions of the temperature profile, the cycle time between consecutive snapshots was set to 7 s. The USAXS images were collected

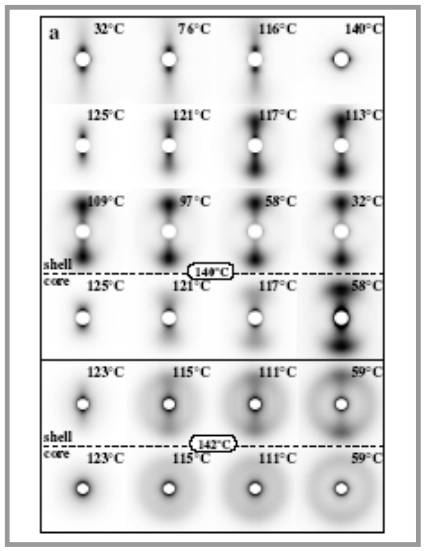


***Figure 1.*** *Polyethylene. SAXS patterns accumulated during melting and recrystallisation of the material as a function of different temperature programs.*

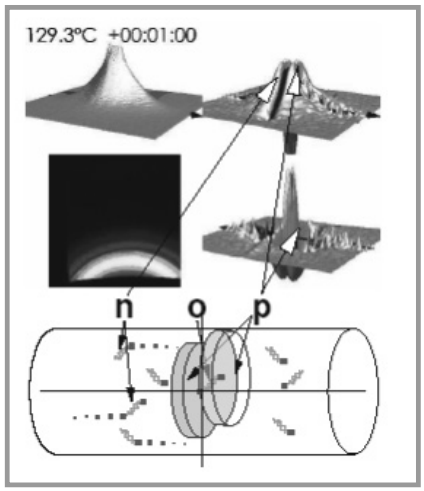


***Figure 2.*** *Crystallisation of an oriented polyethylene melt. 1 min after quenching to 130°C . Top: Movie frame with four panels (left column: SAXS, WAXS, right column: z (r), -z (r)) Bottom: Sketch of the nanostructure. Off-meridional peaks (n) identified as entanglement strands and transverse shift (o) in twin-layers. Layer shape of crystals (p) from meridional peak in z (r) and self-correlation triangle in -z(r).*

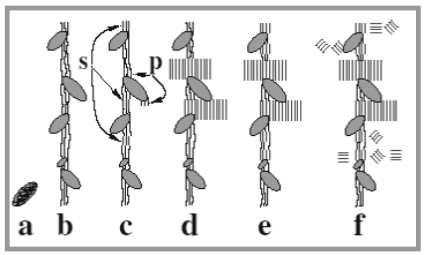


***Figure 3.*** *Principal steps of crystallisation from a highly oriented, quiescent PE melt via a mesophase (a, b, c) coupled to primary (p) and secondary (s) crystal nuclei, extended crystalline layers (d), blocky crystals with longitudinal (e) and lateral (f) correlation.*

by a two-dimensional position sensitive XRII-FReLoN ('Fast Readout, Low Noise') CCD detector developed at ESRF (driven in 1024×1024 pixel mode of 0.164×0.164mm$^2$ each, 14-bit resolution). The sample-to-detector distance was set to 10 m. Wide-angle X-ray scattering (WAXS) was simultaneously recorded using a MCP-Sensicam CCD detector positioned [19, 20] at a short distance from the sample. The SAXS exposure is dynamically adapted during the experiment between 0.1 s and 3 s, in order always to use the full linear range of the detector.

**Data analysis**

Data analysis of the PE data was carried out with computer programs developed under Linux and pv-wave [21] in order to extract information on nanostructure (i.e. a topology $\rho(r)\ \varepsilon\ [\rho_{cryst}, \rho_{amorph}]$ of phases with distinct densities) from two-dimensional (2D) SAXS patterns. The result is an 'edge-enhanced autocorrelation function' z (r) - the autocorrelation of the gradient field $\nabla\rho(r)$. Thus, as a function of the ghost displacement r, the multidimensional chord distribution function (CDF) z (r) shows peaks wherever there are domain surface contacts between the domains in $\rho(r)$ and in its displaced ghost. The CDF with fibre symmetry in real space z ($r_{12}$; $r_3$), was computed from the fibre-symmetric SAXS pattern, I ($s_{12}$; $s_3$), of multi-phase materials with uniaxial orientation [22]. No model is required to compute the CDF. Apart from uniaxial symmetry, we only assume that the nanostructure is sufficiently imperfect. In the historical context, the CDF is an extension of Ruland's interface distribution function (IDF) [23] to the multidimensional case or, in a different view, the Laplacian of Vonk's multidimensional correlation function [24].

## Results and discussion

**Polyethylene**

Figure 1 shows a selection of scattering patterns taken during the non-isothermal crystallisation experiments of PE.

***Melting***

The top row in Figure 1 demonstrates the known melting process [18, 25] of high-pressure injection-moulded PE materials. We observe the typical high long period of 100 nm vanishing. No discrete scattering is observed when the selected melt annealing temperature $T_{max}$ (here 140°C) is reached. After keeping the temperature constant for 2 min, the sample is subjected to cooling at a constant rate of 2°C/min. No change is observed before the temperature drops to 127°C.

***Statistical crystallisation of extended lamellae***

At 125°C (Figure 1, second row, first pattern) we observe the beginning of crystallisation. The perfect orientation of the lamellae is obvious. No reflection maximum is observed, but instead there is an intensity ridge on the meridian. Thus the long period distribution is clearly non-uniform, and the positions at which crystal lamellae are created are almost random.

At 121°C, the length of the intensity ridge has grown far beyond the extension of the discrete scattering found in the original HPIM-PE rod. Still, its 'beam shape' indicates the continued non-uniform long period distribution, now with shorter long periods added. The lateral extension of the crystalline lamellae is still large.

***Correlated crystallisation of imperfect lamellae***

At the ends of the intensity beam, we nevertheless observe the first indications of both a widening, and the creation of an intensity maximum. We conclude that the formation of less extended but more correlated crystallites has begun. Upon continued temperature decrease, more and shorter long periods are added.

Finally, a nanostructure forms that is completely different from that of the original PE rod. Only the perfect orientation is preserved, and in this sense the process is a *re*-crystallisation.

***CDF analysis***

During the PE's crystallisation, we continuously collected very good two-dimensional scattering data automatically transformed into the multidimensional CDF [12, 13, 22]. In order to handle gigabytes of measured 2D patterns, automatic data analysis is the only chance.

Movies prepared after the evaluation show the CDF which can be interpreted and analysed based on its definition. In a first approximation, it shows peaks whereever there are domain surface contacts between domains in $\rho(r)$ and its displaced ghost as a function of ghost displacement. Thus the movies exhibit the

evolution of nanostructure and demonstrate the mechanisms of polymer crystallisation.

Figure 2 shows one movie frame representing the state of an oriented polyethylene (PE) melt to 130°C 1 min after quenching. We observe the primary, extended lamellae (stage 'd' from Fig. 3 which shows sketches of the observed phases of nanostructure evolution). In Fig. 1 the layer character of the crystallites is demonstrated by the fact that the peaks in the CDF are extending in the direction transverse to fibre direction. The small number of peaks shows that only two layers (blue disks in the sketch) are correlated to each other. A transverse offset (p) between the members of the pair of correlated layers is induced by entities of a mesophase.

In conclusion, we find that PE crystallisation is always preceded by a mesophase structure. Based on the structure evolution observed, it is suggested that its entities are entanglement-rich regions and disentangled regions in the melt respectively. Extended lamellae prevail only at high crystallisation temperatures and become more perfect with time. Nevertheless, the majority of ('blocky', cf. Fig. 3e,f) crystallites formed during the final stages of crystallisation are small, imperfect, unoriented, but are located in the centre of free gaps, so that correlations among crystallites are increased.

**Polypropylene**

Figure 4 shows scattering patterns collected in-situ during the melting and crystallisation of highly-oriented PP films. After finding an isotropic SAXS pattern in the melt at different melt-annealing temperatures, oriented crystallisation is observed for melt-annealing temperatures of up to 172°C. Isotropic crystallisation is observed after heating the melt to 180°C. Melt-annealing times were varied between 2 min and 20 min with little effect on recrystallisation after quenching to a crystallisation temperature.

During crystallisation at temperatures of 150°C and 155°C, the material develops a strong equatorial scattering that is not observed when crystallised at higher or lower temperatures. The effect itself can be reproduced. Its strength is variable.

Due to the poor conditions found at BW4 in summer 2004, the intensity was too low to perform quantitative analysis. For the purpose of presentation, the scattering patterns in Figure 4 have been smoothed by the application of a median filter (7×7 pixels).

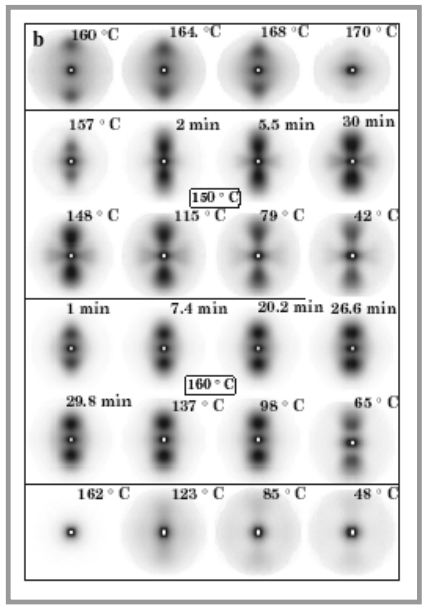


***Figure 4.*** *Hard elastic PP. SAXS patterns accumulated during melting and oriented recrystallisation of the material as a function of different temperature programs. The novel four-point pattern is observed after isothermal crystallisation at 150°C.*

## Conclusions

After comparing the SAXS study results of PP presented first, it has become clear that a state-of-the-art in-situ investigation appears very promising. After such a study, other polymers should also be tested for their ability to crystallise in a highly-oriented state from an oriented melt. By application of this approach, we expect to be able to gather data which results in a very detailed description of the mechanisms that control the formation of crystals in oriented polyolefine melts.

The analysis of the corresponding vast series of two-dimensional scattering data can only be carried out by means of automated data evaluation procedures and is, in general, computationally challenging. Nevertheless, in the field of medical applications, corresponding Fourier analysis methods have become a standard. In material science we are just at the beginning of a period of software engineering that is becoming more and more important as we collect better and better data. As here we have presented nanostructure analysis on perfectly uniaxial materials, the next challenge is already discernible. It will be related to the decomposition of imperfect orientation from nanostructure. Ultimately, the present progress in data analysis is boosted both by theoretical concepts and by the development of powerful synchrotron radiation sources and detectors.


## Acknowledgments

*We thank the Hamburg Synchrotron Radiation Laboratory (HASYLAB) for beam time granted as part of project II-01-041 and the European Synchrotron Radiation Facility (ESRF), Grenoble, for beam time granted as part of project SC 1396. We gratefully acknowledge funding by the Deutsche Forschungsgemeinschaft, project STR 501/4-1.*


## References


1. *Heck B., Hugel T, Iijima M, Sadiku E, Strobl G (1999), New J Phys 1:17.1*
2. *Heck B., Hugel T, Iijima M, Strobl G (2000), Polymer 41:8839*
3. *Heeley E.L., Maidens A.V., Olmsted P.D., Bras W., Dolbnya I.P., Fairclough J.P.A., Terrill N.J., Ryan A.J., (2003), Macromolecules 36:3656*
4. *Bras W., Dolbnya I., Detollenaere D., van Tol R., Malfois M., Greaves G., Ryan A., Heeley E. (2003), J Appl Cryst 36:791*
5. *Somani R.H., Yang L., Hsiao B.H., Fruitwala H. (2003), J Macromol Sci Part B Phys B42:515*
6. *Somani R.H., Yang L., Hsiao B.S., Agarwal P.K., Fruitwala H.A., Tsou A.H. (2002), Macromolecules 35:9096*
7. *Yamazaki S., Hikosaka M., Toda A., Wataoka I., Yamada K. Tagashira K. (2003), J Macromol Sci Part B Physics B42:499*
8. *Stribeck N. (2003), Fibr Text EE 11:33*
9. *Pearce R., Vancso G.J. (1998), Polymer 39:1237*
10. *Hobbs J.K., Humphris A.D.L., Miles M.J. (2001), Macromolecules 34:5508*
11. *Humphris A.D.L., Hobbs J.K., Miles M.J. (2003), Appl Phys Lett 83:6*
12. *Stribeck N., Bayer R., Bösecke P., Almendarez Camarillo A. (2004). Polymer submitted*
13. *Stribeck N., Bösecke P., Bayer R., Almendarez Camarillo A (2004), Progr Coll Polym Sci in print*
14. *Stribeck N., Almendarez Camarillo A., Cunis S., Bayer R.K., Gehrke R. (2004), Macromol Chem Phys 205:1445*
15. *Stribeck N. (2004), Macromol Chem Phys 205:1455*
16. *Stribeck N., Almendarez Camarillo A, Bayer R (2004), Macromol Chem Phys 205:1463*
17. *Noether H.D. (1979), Intern J Polymeric Mater 7:57*
18. *Stribeck N., Bayer R., von Krosigk G., Gehrke R. (2002), Polymer 43:3779*
19. *Bösecke P., Diat O. (1997), J Appl Cryst 30:867*
20. *Urban V., Panine P., Ponchut C., Bösecke P,. Narayanan T. (2001), J Appl Cryst 36:809*
21. *pv-wave, version 7.5 (2001),, Visual Numerics Inc., Boulder, Colorado*
22. *Stribeck N. (2001), J Appl Cryst 34:496*
23. *Ruland W. (1977), Colloid Polym Sci 255:417*
24. *Vonk C.G. (1979), Colloid Polym Sci 257:1021*
25. *Rueda D.R., Ania F., Baltá Calleja F.J. (1997), Polymer 38:2027*


***Received 08.12.2004 Reviewed 10.02.2005***